

# Accelerated carcinogenesis following liver regeneration is associated with chronic inflammation-induced double-strand DNA breaks

Hila Barash<sup>a,b</sup>, Eitan R. Gross<sup>c</sup>, Yifat Edrei<sup>a,b</sup>, Ezra Ella<sup>a</sup>, Ariel Israel<sup>a</sup>, Irit Cohen<sup>a</sup>, Nathalie Corchia<sup>a,b</sup>, Tehila Ben-Moshe<sup>a</sup>, Orit Pappo<sup>d</sup>, Eli Pikarsky<sup>d</sup>, Daniel Goldenberg<sup>a</sup>, Yosef Shiloh<sup>e</sup>, Eithan Galun<sup>a</sup>, and Rinat Abramovitch<sup>a,b,1</sup>

<sup>a</sup>The Goldyne Savad Institute of Gene Therapy, <sup>b</sup>Magnetic Resonance Imaging/Magnetic Resonance Spectroscopy Laboratory, Human Biology Research Center, and Departments of <sup>c</sup>Pediatric Surgery and <sup>d</sup>Pathology, Hadassah Hebrew University Medical Center, Jerusalem, Israel; and <sup>e</sup>The David and Inez Myers Laboratory for Cancer Research, Department of Human Molecular Genetics and Biochemistry, Sackler School of Medicine, Tel Aviv University, Israel

Edited by Bert Vogelstein, The Sidney Kimmel Comprehensive Cancer Center at The Johns Hopkins University, Baltimore, MD, and approved December 22, 2009 (received for review August 5, 2009)

Hepatocellular carcinoma (HCC) is the third leading cause of cancer mortality worldwide and is considered to be the outcome of chronic liver inflammation. Currently, the main treatment for HCC is surgical resection. However, survival rates are suboptimal partially because of tumor recurrence in the remaining liver. Our aim was to understand the molecular mechanisms linking liver regeneration under chronic inflammation to hepatic tumorigenesis. Mdr2-KO mice, a model of inflammation-associated cancer, underwent partial hepatectomy (PHx), which led to enhanced hepatocarcinogenesis. Moreover, liver regeneration in these mice was severely attenuated. We demonstrate the activation of the DNA damage-response machinery and increased genomic instability during early liver inflammatory stages resulting in hepatocyte apoptosis, cell-cycle arrest, and senescence and suggest their involvement in tumor growth acceleration subsequent to PHx. We propose that under the regenerative proliferative stress induced by liver resection, the genomic unstable hepatocytes generated during chronic inflammation escape senescence and apoptosis and reenter the cell cycle, triggering the enhanced tumorigenesis. Thus, we clarify the immediate and long-term contributions of the DNA damage response to HCC development and recurrence.

hepatocellular carcinoma | MRI | MDR2<sup>-/-</sup> mice | genomic instability

The inflammatory process is a contributor, if not a cause, of a wide variety of neoplasms (1). It is estimated that underlying inflammatory responses are linked to 15–20% of all deaths from cancer worldwide (2). Whereas the association between chronic immune activation and the development of cancer has been recognized for some years, only recently have we begun to understand the mechanisms underlying this phenomenon (3–5). Hepatocellular carcinoma (HCC) is the fifth most common cancer worldwide (6). It has become widely recognized that the most influential factor for the development of HCC is ongoing inflammation in the liver induced by chemicals, viral or bacterial infections, autoimmunity, and metabolic diseases (7). The role of transcription factors such as NF- $\kappa$ B and STAT3, cytokines like IL-6 and IL-1 $\alpha$ , ligands of the EGF receptor, and other inflammatory mediators in HCC development have been described previously (8, 9).

Liver resection [partial hepatectomy (PHx)] is the preferred treatment for HCC patients. However, survival rates following PHx are suboptimal, mostly because of tumor recurrence, which, within 5 years, is in the range of 75–100% of cases (10, 11). Undetected intrahepatic lesions attribute to 60–70% of recurrences, whereas 30–40% are de novo HCCs (12).

Previous animal studies investigating the effects of liver regeneration on tumor progression were performed using tumor cells transplanted s.c. or directly into the liver (13, 14) or on chemically induced tumors (15–17). Additional molecular studies were based on plasma injection or in vitro experiments (13, 15). In these animal models, PHx has been shown to enhance both the initiation

and promotion phases of hepatocarcinogenesis when compared with sham operation (13, 16–19). However, in these models, there was no underlying liver inflammation, as is the case in humans with HCC. Currently, there is insufficient information on the mechanisms by which the inflammatory microenvironment affects liver regeneration and the effect of both inflammation and regeneration on hepatocarcinogenesis. Under these conditions, there is replicative senescence exhaustion in the cirrhotic liver, increasing the risk for malignancy (20). Previous studies have revealed inhibition of liver regeneration in mice bearing transplanted tumors or injected i.p. with plasma from tumor-bearing mice (21, 22).

Our research objective was to understand the biological processes that could promote the development of HCC in a chronically inflamed liver during regeneration. To study the mutual effects of liver regeneration, inflammation, and carcinogenesis, we used the Mdr2-KO (Mdr2<sup>-/-</sup>) mouse, which is an HCC model simulating the human clinical condition (i.e., HCC resulting from chronic liver inflammation) (23). These mice lack the liver-specific P-glycoprotein inducing portal inflammation at an early age (3 months), which is followed by slowly developing HCC (between the ages of 12 and 15 months).

In previous studies, we followed the development of liver fibrosis and determined the role of inflammation in the development of HCC in these mice (9, 24–26). In this study, we aimed to assess the impact of regenerative stress during chronic liver inflammation on carcinogenesis. We have observed that liver resection significantly promotes tumorigenesis and attenuates regeneration. We propose that under the regenerative proliferative stress induced by liver resection, the genomic unstable hepatocytes generated during chronic inflammation escape senescence or apoptosis and reenter the cell cycle, triggering the enhanced tumorigenesis.

## Results

**Liver Regeneration Accelerates Tumorigenesis.** To study the effects of liver regeneration on hepatocarcinogenesis in a chronic inflamed liver, we performed PHx or sham surgery on 3-month-old

Author contributions: H.B., E.G., and R.A. designed research; H.B., E.R.G., Y.E., E.E., I.C., N.C., T.B.-M., and R.A. performed research; H.B., Y.E., A.I., O.P., E.P., D.G., and R.A. analyzed data; and H.B., D.G., Y.S., E.G., and R.A. wrote the paper.

The authors declare no conflict of interest.

This article is a PNAS Direct Submission.

Freely available online through the PNAS open access option.

Data deposition: The data reported in this paper have been deposited in the Gene Expression Omnibus (GEO) database, [www.ncbi.nlm.nih.gov/geo](http://www.ncbi.nlm.nih.gov/geo) (accession no. GSE14539) (National Center for Biotechnology Information tracking system no. 15577663).

<sup>1</sup>To whom correspondence should be addressed at: Hadassah Hebrew University Medical Center, PO Box 12000, Jerusalem 91120, Israel. E-mail: [rinat@hadassah.org.il](mailto:rinat@hadassah.org.il).

This article contains supporting information online at [www.pnas.org/cgi/content/full/0908867107/DCSupplemental](http://www.pnas.org/cgi/content/full/0908867107/DCSupplemental).

(inflamed liver) and 9-month-old (preneoplastic stages) *Mdr2*<sup>-/-</sup> mice (Fig. S1 A and B). Tumor progression was enhanced in the PHx *Mdr2*<sup>-/-</sup> mice compared with sham operated *Mdr2*<sup>-/-</sup> mice, as monitored by MRI, regardless of age at surgery (Fig. 1 and Fig. S2). The tumors were distinguishable by MRI at least a month earlier in the PHx mice compared with the sham operated *Mdr2*<sup>-/-</sup> mice. In mice operated on at the age of 9 months, both the size and number of tumors increased in the PHx group compared with the sham group (Fig. 1C). Although tumors from both PHx- and sham-operated groups were defined as well-differentiated HCC by pathological examination, a larger number of mitotic cells were present in tumors of PHx mice (25 ± 5 vs. 5 ± 3, respectively), corresponding to the MRI results. These results might suggest a direct or indirect effect of the growth factors and cytokines, which are involved in the regeneration process, on the preneoplastic liver parenchyma. However, PHx had a prolonged effect on tumor growth in view of the fact that tumor size was also enhanced in the 3-month-old *Mdr2*<sup>-/-</sup> mice that underwent surgery (Fig. 1D).

***Mdr2*<sup>-/-</sup> Mice Regenerative Delay.** Because inflammatory mediators play an important role in liver regeneration and there is a known elevation of the mitotic index in the *Mdr2*<sup>-/-</sup> mice (26), one would expect enhanced liver regeneration following PHx in these mice. We subjected 3-month-old (chronic inflammation) and 9-month-old (preneoplastic stages) *Mdr2*<sup>-/-</sup> and equivalent control mice to 70% PHx and analyzed the regenerative response of the liver using serial MRI scans. Surprisingly, liver regeneration was significantly delayed in the *Mdr2*<sup>-/-</sup> mice compared with controls at both ages (*P* < 0.05 for the 3-month-old mice and *P* < 0.01 for the 9-month-old mice; Fig. 2). The livers of the *Mdr2*<sup>-/-</sup> mice reached their original volume 2 weeks post-PHx compared with 7 days in the control mice (Fig. 2 C and D).

We continued to unfold the molecular mechanisms responsible for the regeneration attenuation on inflammation only in

the 9-month-old mice. We evaluated hepatocyte proliferation kinetics using injections of BrdU (staining cells entering S-phase) at several time points (days 2, 4, 6, 9, and 12) post-PHx. Measurements done in the control mice yielded, as expected, an increase in the number of BrdU-labeled hepatocytes on days 4–6 post-PHx (aged mice; Fig. 2E). In the *Mdr2*<sup>-/-</sup> mice, however, only a few BrdU-labeled hepatocytes were observed at any of the time points measured (*P* < 0.001). We further checked whether the hepatocytes had entered the cell cycle by immunostaining with CDC47/MCM7 (detecting cells mainly in the G<sub>1</sub>-phase)

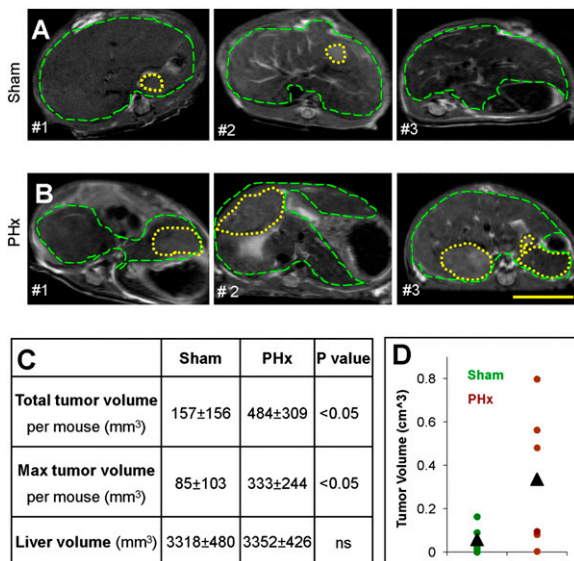


**Fig. 1.** Tumorigenesis acceleration. Representative T<sub>2</sub>-weighted axial MRI of three different *Mdr2*<sup>-/-</sup> mice per group aged 12 months that underwent sham surgery (A) or PHx (B) at the age of 9 months. Dashed green lines encircle the liver, and yellow dotted lines encircle tumors. (Scale bar: 1 cm.) (C) Table summarizing the tumor status at the age of 12 months of mice that underwent sham surgery (*n* = 5) or PHx (*n* = 10) at the age of 9 months, as assessed by MRI. (D) Liver tumor volume in *Mdr2*<sup>-/-</sup> mice operated on at the age of 3 months was assessed at the age of 12 months and plotted for each animal and for the group average of sham surgery (green, *n* = 5) or PHx (brown, *n* = 6) (*P* < 0.05).

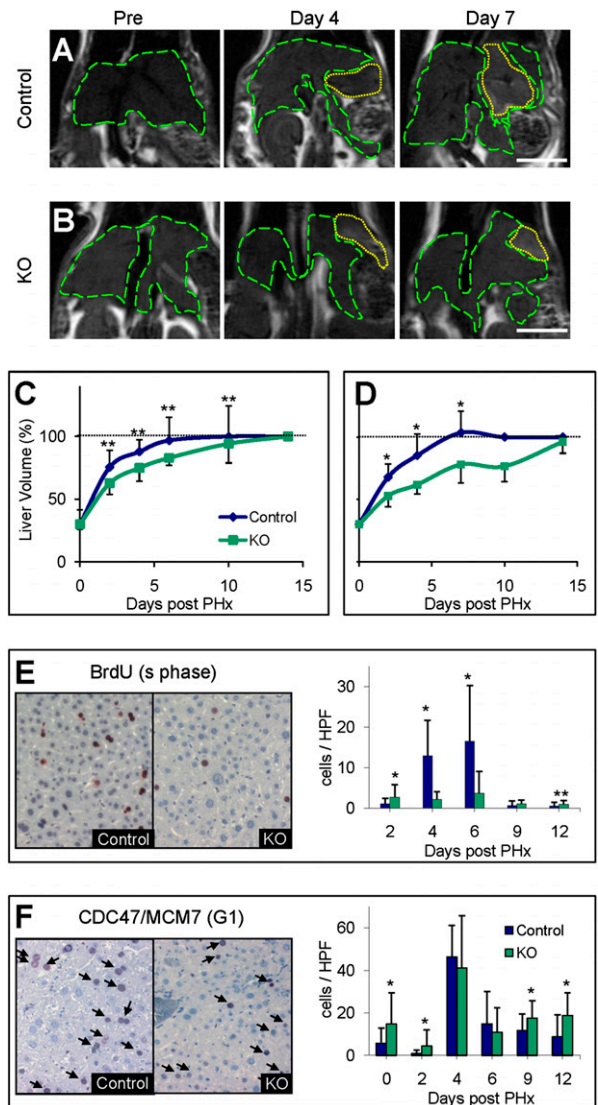


**Fig. 2.** Regenerative delay. Representative anatomical coronal MRI of the same 9-month-old control (A) and *Mdr2*<sup>-/-</sup> (KO) (B) mice before and on days 4 and 7 following PHx. Dashed green lines encircle the liver, and yellow dotted lines encircle the residue of the resected lobe. (Scale bar: 1 cm.) Liver volume monitoring after 70% PHx of 3-month-old (*n* = 8 per time point per group) (C) and 9-month-old (*n* ≥ 10 per time point per group) (D) in control (blue) and KO (green) mice. Percentage of liver volume compared with the volume before surgery was calculated for each animal, and averages ± SD were plotted. \**P* < 0.01; \*\**P* < 0.05. The horizontal dashed line marks liver volume restoration. Representative liver sections of control and KO 9-month-old mice killed on day 6 after 35% PHx immunostained for BrdU (E) and CDC47 (F). Quantification of the BrdU- and CDC47-positive cells (E and F, respectively) was done at the indicated time points for 30 randomly selected fields (*n* ≥ 3 mice per time point per group). HPF, high-power field.

(Fig. 2F). Surprisingly, in the 9-month-old  $Mdr2^{-/-}$  mice, a larger number of hepatocytes were found to be CDC47-positive (Fig. 2F), indicating that they had entered the cell cycle. Hence, these results suggest that in the  $Mdr2^{-/-}$  mice, a significant number of hepatocytes entered the cell cycle but did not progress into DNA synthesis and cell division, resulting in a proliferative delay.

**Gene Expression Signature During Regeneration in an Inflamed Liver.** To reveal the molecular basis for the enhanced tumorigenesis and the delayed regeneration in the PHx  $Mdr2^{-/-}$  mice, we performed genome-scale gene expression profiling to compare expression patterns of liver samples of 9-month-old  $Mdr2^{-/-}$  and control mice from days 0 (the removed lobe), 2, and 6 post-PHx (Fig. S3A). A bioinformatics/statistical analysis revealed a dramatic up-regulation of genes in the control mice on day 2 or 6 post-PHx (>300 genes) compared with day 0 when stringent criteria were applied (Fig. S3B and C). This up-regulation of genes, attributable to liver regeneration, was scarce in the  $Mdr2^{-/-}$  mice. Remarkably, most of the genes that were up-regulated in the control mice post-PHx were not up-regulated in the  $Mdr2^{-/-}$  mice before PHx [Gene Expression Omnibus (GEO) accession no. GSE14539]. Subsequently, we reviewed the annotation groups of the up-regulated genes. Control mice demonstrated an up-regulation of genes known to be involved in cell cycle, cell death, and DNA damage on day 6 post-PHx, which was absent in the  $Mdr2^{-/-}$  mice (Fig. 3A and B).

In the 9-month-old  $Mdr2^{-/-}$  mice, we found abnormal expression levels of genes involved in DNA repair and, specifically, members of the ataxia telangiectasia mutated (ATM)/ATM-RAD3 related (ATR) pathway that are involved in the cellular response to DNA double-strand breaks (DSBs) (Fig. 3C). Genes involved in DNA damage sensing and mediators of the damage signal, including BRCA1, Cdkn1a, H2afx, and Trp53bp1, were a priori up-regulated in  $Mdr2^{-/-}$  mice on day 0.

**High Incidence of DNA Damage in the  $Mdr2^{-/-}$  Mice.** Because we found up-regulation of DNA damage and repair genes in the  $Mdr2^{-/-}$  mice, we examined the presence of DNA damage in their livers using two markers of DSBs: nuclear foci of the protein 53BP1, which accumulates at DSB sites (27), and phosphorylation of the histone H2AX by antibodies against the phosphorylated histone ( $\gamma$ -H2AX) (28). In the control mice, hardly any  $\gamma$ -H2AX-labeled hepatocytes were observed (Fig. 4A). However, there were significantly more  $\gamma$ -H2AX-labeled hepatocytes in  $Mdr2^{-/-}$

mice ( $P < 0.001$ ; Fig. 4A). Moreover, 53BP1 exhibited nuclear foci in many hepatocytes of  $Mdr2^{-/-}$  mice (Fig. S4). Thus, two indicators of DSBs suggest the presence of DSBs in 9-month-old  $Mdr2^{-/-}$  mice.

**Activation of DNA Damage Downstream Effectors.** The DSB response begins with the recruitment of the sensor proteins to the damaged sites (29). These proteins are involved in the initial processing of the damage and activation of the transducers of the DNA damage alarm. The primary transducer of the DSB alarm is the nuclear serine-threonine kinase ATM (30). ATM then phosphorylates a plethora of effectors, which are key players in a variety of damage response pathways (30, 31), including DNA repair, cell cycle checkpoints, and programmed cell death (32, 33). Activated ATM phosphorylates, among others, the checkpoint protein kinase Chk2 on T68 (33, 34). Indeed, Chk2 was phosphorylated in many of the hepatocytes of 9-month-old  $Mdr2^{-/-}$  mice but not in controls, as seen by immunohistochemistry ( $P < 0.001$ ; Fig. 4B). Thus, the high level of DSBs in the  $Mdr2^{-/-}$  hepatocytes induced activation of the DNA damage-response pathway.

**DNA Damage-Response Targets.** To determine the physiological consequences of up-regulation of the DNA damage sensors and mediator responses, we further explored the status of the end points of the damage response. Following DNA damage, normal cells arrest at the  $G_1/S$  or  $G_2/M$  transition of the cell cycle. Indeed, p21, a major cell cycle inhibitor at both  $G_1$  and  $G_2$  (35), was significantly elevated in the  $Mdr2^{-/-}$  mice, as indicated by the gene expression profiles and confirmed by immunohistochemistry ( $P < 0.001$ ; Fig. 4C). The  $G_2$  arrest is thought to occur by mechanisms that maintain inhibitory phosphorylation on Thr14 and Tyr15 of Cdk1 (36). Thus, we examined samples of liver sections for Tyr15-phosphorylated Cdk1 (pY-Cdk1). In the 9-month-old  $Mdr2^{-/-}$  mice, pY-Cdk1 staining was predominantly cytoplasmic and mainly in the vicinity of blood vessels (Fig. 4D). In control mice, we found significantly fewer pY-Cdk1-positive cells, with complete abolition of phosphorylation on day 6 post-PHx in contrast to the  $Mdr2^{-/-}$  mice ( $P < 0.01$ ; Fig. 4D). Moreover, there was a remarkable increase of senescent hepatocytes, an indicator of long-term cell cycle arrest (37), in aged  $Mdr2^{-/-}$  mice as assessed by both  $\beta$ -galactosidase expression and heterochromatin protein-1 (HP1) immunohistochemical staining (Fig. S5). Furthermore, there was an apparent elevation of apoptosis in the  $Mdr2^{-/-}$  mice

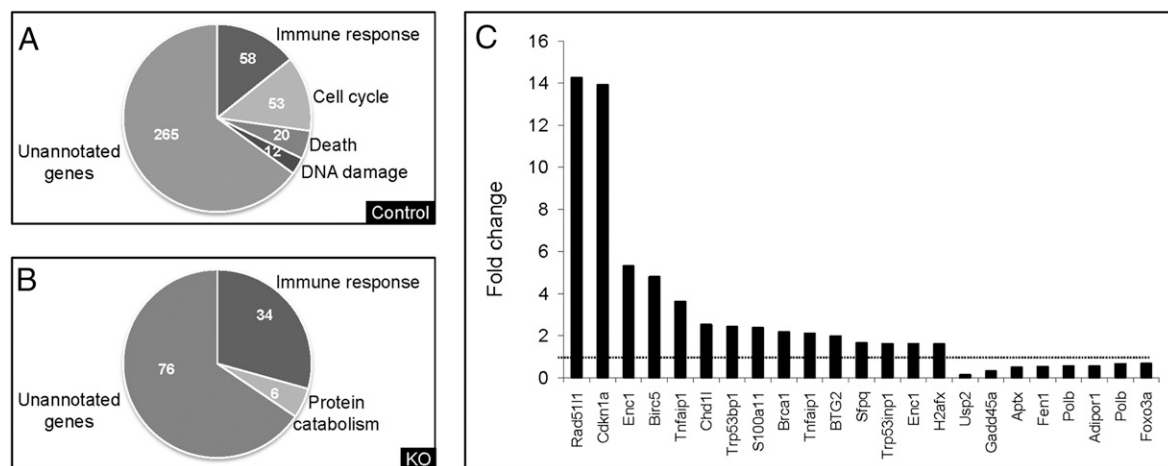


**Fig. 3.** Gene expression profile. Control or  $Mdr2^{-/-}$  (KO) livers of 9-month-old mice that underwent PHx were analyzed by Affymetrix arrays. Functional analysis of the up-regulated genes on day 6 after PHx in control (A) or KO (B) mice. (C) Graph illustrating the fold change in gene expression of representative differentially regulated genes involved in DNA damage and repair between KO vs. control mice before PHx. The horizontal dashed line marks a fold change of 1 (no change).

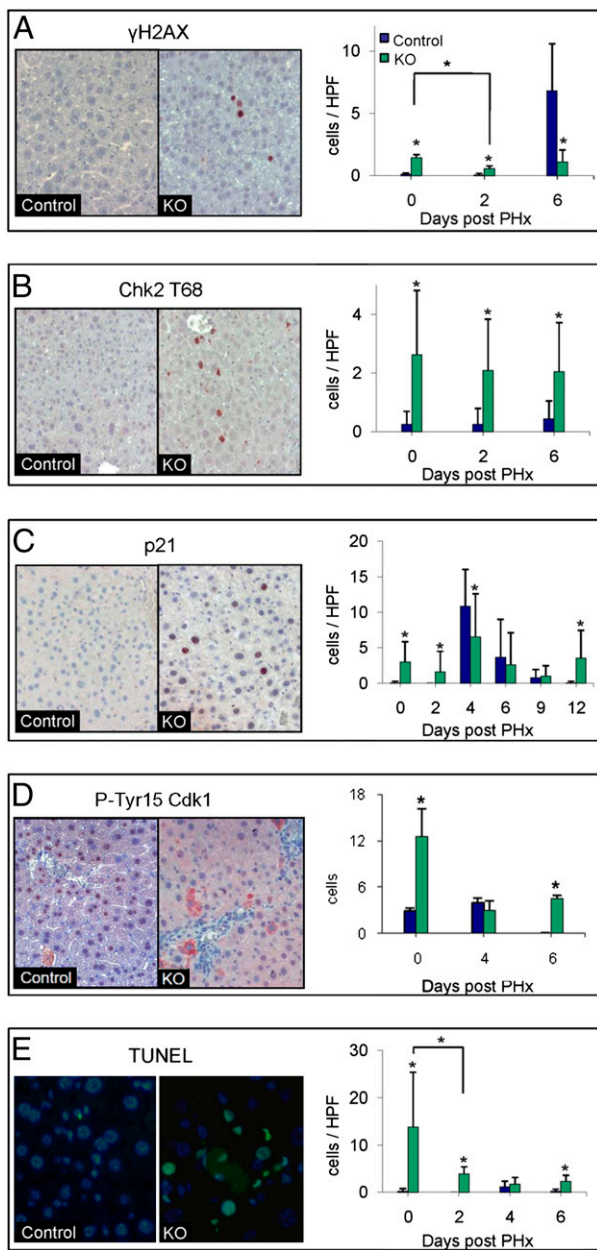


**Fig. 4.** Activation of DNA damage response. Representative liver sections of 9-month-old control and *Mdr2*<sup>-/-</sup> (KO) mice obtained before PHx. Slides were immunostained (red) for  $\gamma$ -H2AX (A), Chk2-T68 (B), P21 (C), and Tyr15-phosphorylated Cdk1 (D) and for apoptosis by TUNEL assay (E). (DAPI, blue; apoptosis, green). Quantification of immunostaining for all time points of  $\gamma$ -H2AX (A), Chk2-T68 (B), P21 (C) and p-Tyr15 Cdk1 (D) and for apoptosis (E) was done ( $n \geq 30$  per time point per group,  $*P < 0.001$ ). HPF, high-power field.

as identified by both gene expression and histological studies. Cluster analysis of proapoptotic genes demonstrated elevation of the expression of these genes in the *Mdr2*<sup>-/-</sup> mice (Fig. S6), and there was a significantly higher level of TUNEL staining in the *Mdr2*<sup>-/-</sup> mice compared with control mice ( $P < 0.001$ ; Fig. 4E). In conclusion, the hepatocytes of the *Mdr2*<sup>-/-</sup> mice contained high levels of DSBs inducing the DNA damage response, which, in turn, stimulated both cell cycle arrest and apoptosis.

**Genomic Instability.** DSBs constitute a major threat to genome integrity because they can result in chromosomal aberrations leading to cell malfunctioning, uncontrolled replication, and cell

death (38). Thus, we investigated whether genomic instability had occurred in the *Mdr2*<sup>-/-</sup> mice. Indeed, many genes in the recently published chromosomal instability gene expression signature (39) were significantly elevated ( $P < 0.01$ ) in the 9-month-old *Mdr2*<sup>-/-</sup> mice compared with control mice (Fig. S7). Of the 53 signature genes identified in our probe set, 25 were up-regulated in the *Mdr2*<sup>-/-</sup> mice, demonstrating enrichment of these genes. Thus, there was apparent genomic instability in the livers of the 9-month-old *Mdr2*<sup>-/-</sup> mice before PHx. To assess global genomic changes directly, we performed comparative genomic hybridization (CGH) analysis of four HCC tumors and their matched non-tumorous liver samples from 9-month-old *Mdr2*<sup>-/-</sup> mice that underwent PHx at the age of 6 months, using an Agilent 44K array CGH platform. The CGH results demonstrated prolonged amplification in all four tumors with no detectable deletion (Fig. S8). In two of four tumors, there were regions that were amplified by 2- to 12-fold, which could indicate clonality. Three chromosomal regions were amplified in three (75%) of the four tumors, possibly indicating unknown fragile sites in mice. We found good correlation between tumor size and fold change of the amplified regions (Fig. S9A). At least two of the common amplified regions in tested murine HCC tumors had synteny to chromosomal regions that are frequently amplified in human HCC (Fig. S9B).

### Discussion

Inflammation is a common theme across many of the HCC etiologies (40). *Mdr2*<sup>-/-</sup> mice offer a model that recapitulates key features of the human disease, including inflammatory environment, genomic instability, and fibrosis (9, 23, 24, 26). Using this model, we explored the interaction between inflammation, regeneration, and HCC and propose a molecular explanation for the enhanced liver tumorigenesis following PHx. We found accelerated tumorigenesis in the *Mdr2*<sup>-/-</sup> hepatectomized mice. This effect was not only immediate but lasting, because PHx performed on 3-month-old mice also resulted in enhancing the development of HCC. Thus, PHx and liver regeneration in an inflammatory environment induce permanent alterations in the liver contributing to carcinogenesis.

We revealed attenuated regeneration in the *Mdr2*<sup>-/-</sup> mice. In addition, we demonstrated that hepatocyte proliferation was decelerated in these 9-month-old mice, as previously found in 3-month-old mice (26). In the *Mdr2*<sup>-/-</sup> mice, a significant number of hepatocytes entered the cell cycle but did not progress into DNA synthesis and cell division, culminating in a proliferative delay. There may be many explanations for this delay, among which are up-regulation of p21; maintenance of the inhibitory phosphorylation on Tyr15 of Cdk1; and up-regulation of TGF- $\beta$ 1, which is known to control and terminate regeneration (41). Evidently, in the array analyses, we identified high expression of the TGF- $\beta$ 1 receptor and p21 in the *Mdr2*<sup>-/-</sup> mice and further confirmed these findings by immunostaining for p21 and pY-Cdk1.

Using gene expression profiling and immunostaining, we discovered abnormal expression of DNA damage-response genes in the *Mdr2*<sup>-/-</sup> mice (i.e.,  $\gamma$ -H2AX, 53BP1, and Chk2). Therefore, we propose that there is an accumulation of DSBs in the hepatocytes of the *Mdr2*<sup>-/-</sup> mice consequential to the chronic inflammatory state. MiR-34a is directly transactivated by p53 and induces apoptosis and cell cycle arrest in the G<sub>1</sub>-phase, thereby suppressing tumor cell proliferation and DNA repair (42). We found up-regulation of miR-34A in 9-month-old *Mdr2*<sup>-/-</sup> mice, supporting our conclusion that the DNA damage-response pathway is activated in these mice (see SI Text). Moreover, we revealed three end points of the DNA damage response in these hepatocytes: high levels of cell cycle arrest, senescence, and apoptosis. The cell cycle arrest explains the delayed regeneration and the hepatocytes' failure to complete the cell cycle and liver volume. There is apparent apoptosis of hepatocytes in the 9-month-old *Mdr2*<sup>-/-</sup> mice before PHx, declining following PHx,

probably attributable to factors known to provide protection from apoptosis during liver regeneration (43). Hence, hepatocytes destined to undergo apoptosis or under senescence because of DSBs are salvaged and contribute to the genomic instability state of the liver.

Inflammatory promoters increase production of reactive oxygen species, leading to oxidative DNA damage, and reduce DNA repair (5). Leukocytes and other phagocytic cells induce DNA damage in proliferating cells through their generation of reactive oxygen and nitrogen species that are produced normally by these cells to fight infection (5). It has been found previously that inflammation engages components of the DNA damage-response machinery through oxidative stress (34, 44). Moreover, there is some preliminary evidence for elevated oxidative stress in the *Mdr2*<sup>-/-</sup> mice in the chronic inflammatory stages (26). Furthermore, intrahepatic chronic hypoxia may occur during the inflammatory and fibrotic processes that characterize several chronic liver diseases (45). Hypoxic cells may have decreased DNA repair and increased chromosomal instability (46). Migration inhibitory factor is involved in modulation of the DNA damage response during inflammation and is up-regulated in the *Mdr2*<sup>-/-</sup> mice. In summary, it is not surprising that the chronically inflamed and fibrotic liver of *Mdr2*<sup>-/-</sup> mice suffering from oxidative stress exhibits an activated DNA damage response.

PHx in the *Mdr2*<sup>-/-</sup> mice induces a replicative stress that is initially halted, thus attenuating regeneration. Cell proliferation involves numerous processes that need to be tightly coordinated to ensure the preservation of genome integrity and to promote faithful genome propagation. Coordination of DNA replication with DNA damage sensing and repair and cell cycle progression ensures, with a high probability, genome integrity during cell division, thus preventing mutations and DNA rearrangements (47). Under replication stress, ssDNA gaps and DNA breaks can occur (47), as mirrored by the up-regulation in control mice of the genes included in the chromosomal instability signature (39) during regeneration (Fig. S6). Up-regulation of the chromosomal instability signature genes suggests genomic instability in the livers of the 9-month-old *Mdr2*<sup>-/-</sup> mice before PHx.

Inaccurate DNA repair can lead to mutations and/or chromosomal aberrations that can contribute to carcinogenesis (36, 38). During tissue injury, cell proliferation is enhanced while the tissue regenerates; proliferation and inflammation subside after the repair is completed. In contrast, proliferating cells that sustain DNA damage and/or mutagenic assault, such as the resected livers in an inflammatory background, continue to proliferate in microenvironments rich in inflammatory cells and growth/survival factors that support their growth (5). Additionally, some of the inflammation-induced DNA damaged cells under proliferative stress replicate, leading to increased genomic instability and facilitating tumorigenesis (Fig. 5 and Fig. S8).

It has been demonstrated previously that defects in DSB repair lead to chromosomal instability (48). In humans, up-regulation of DNA repair genes in cirrhotic patients was identified. Increased DNA repair activity in cirrhosis with inflammatory activity may reflect increased DNA damage as a consequence of chronic liver injury (49). Activation of the ATM signaling pathway was found in chronic nonsupportive destructive cholangitis in primary biliary cirrhosis (50). Signs of endogenous DNA damage, marked by Chk2 phosphorylation and  $\gamma$ -H2AX, were found in the cancerous portions of histological sections (34). Additionally, genomic instability is a common feature of human HCC, with various mechanisms suspected to contribute, including telomere erosion, chromosomal segregation defects, and alterations in the DNA damage-response pathways (40). There are many genomic alterations in HCC, as evidenced by CGH studies (40). Recently, it has been shown in *Ku70*<sup>-/-</sup> mice that defective DNA repair induces chromosomal instability accelerating liver carcinogenesis (51).

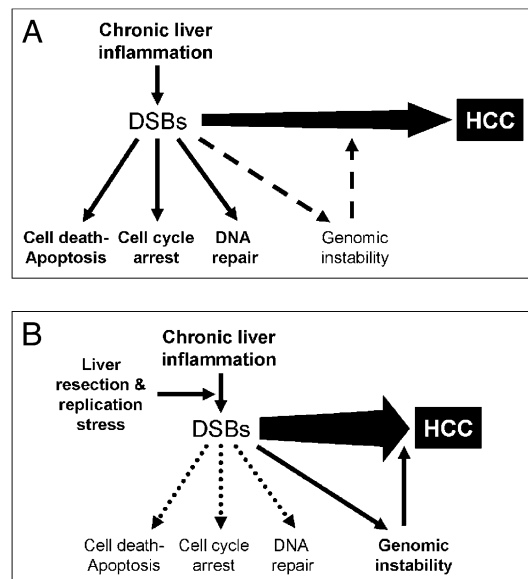


**Fig. 5.** Genomic instability. Proposed model to the enhanced tumorigenesis induced by liver resection under chronic inflammatory background. (A) Chronic liver inflammation induces many afflictions, including DSBs, by oxidative damage. All these ailments, together and apart, contribute to the progress of HCC. The DNA damage response leads to cell cycle arrest, DNA repair, and apoptosis (solid-line arrows). Accumulation of DNA damage results in genomic instability (dashed-line arrow). (B) While performing liver resection, we induced proliferative stress on the hepatocytes. Under the replicative stress, some of the impaired cells containing DSBs were salvaged from the DNA damage response and replicated, thus increasing genomic instability and facilitating tumor progression (solid-line arrow).

Our data suggest that before PHx, there is genomic instability in the hepatocytes of the *Mdr2*<sup>-/-</sup> mice induced by the activated DNA damage response. It is apparent that the DNA damage response has a role as a barrier in tumor progression and that replication stress is an underlying trigger of oncogene-induced DNA damage response (52, 53). The proliferative stress during liver regeneration on the mutated hepatocytes may explain the enhanced tumorigenesis. DNA damage-response-induced genomic instability may lead to loss of tumor suppressors and oncogene activation. The observation that a chronic inflammatory state is a prerequisite for genomic instability, leading to HCC on enhanced regeneration, should warrant further investigations aimed at suppressing the inflammatory stress long before the development of dysplastic changes. In addition, to reduce tumor recurrence following liver resection, administration of pro-DNA repair agents should be considered before resection.

## Materials and Methods

**Mice.** Founders of the FVB.129P2-Abcb4<sup>tm1Bor</sup> (*Mdr2*<sup>-/-</sup>; formerly FVB.129P2-Pgy24<sup>tm1Bor</sup>) and WT FVB/NJ mice were purchased from the Jackson Laboratory. The F1 hybrids produced by breeding of FVB.129P2-Abcb4<sup>tm1Bor</sup> and FVB/NJ mice were used as age-matched controls.

Thirty-five percent and 70% PHx or sham surgery was performed according to the method of Higgins and Anderson (54), adapted to mice (55), on 3-month-old (inflamed liver), 6-month-old, and 9-month-old (preneoplastic stages) *Mdr2*<sup>-/-</sup> mice and aged-matched control mice (Fig. S1).

**Gene Expression Profiling.** RNA was isolated from frozen liver samples of 9-month-old *Mdr2*<sup>-/-</sup> and control mice obtained on days 0 (the removed lobe), 2, and 6 following PHx (Figs. S1B and S3). Total RNA was isolated and subjected to genome-scale gene expression profiling using Mouse Genome Array 430A (Affymetrix, Inc.). The gene expression data discussed in this article were deposited in the National Center for Biotechnology Information's (NCBI) GEO Series (accession no. 14539) and are accessible through the NCBI tracking system (no. 15577663).

**Immunohistochemistry.** The following antibodies were used for immunohistochemistry: mouse antibody to CDC47 (1:100; Biocare Medical), mouse antibody to  $\gamma$ -H2AX (1:100, 05-636; Upstate), rabbit antibody to Chk2-T68 (1:50; Abcam), mouse antibody to P21 (1:500, sc-6246; Santa Cruz), and rabbit antibody to CDC2 phospho-(Tyr15) (1:50, Novus Biologicals). BrdU staining was performed using a Cell proliferation kit (Amersham). TUNEL staining was performed with an in situ Cell Death Detection Kit (Roche Diagnostics). A detailed description of all the other methods appears in *SI Materials and Methods*.

**ACKNOWLEDGMENTS.** We thank Mery Clausen for assisting in manuscript editing and Reba Condiotti for assisting in DNA extraction for CGH analysis. This

research was supported in part by Grant 728/05 from the Israel Science Foundation (to R.A.); the Israeli Science Foundation (E. G.); the Israeli Ministry of Science through a grant from the National Gene Therapy Knowledge Center and through Grants LSHB-CT-2004-512034 (MOLEDA), LSHB-CT-2005-018961 (INTHER), and the FP7 program LSHB-CT-2008-223317 (LIV-ES) (to E. G.); and the Kamea Scientific Foundation of the Israeli Government (D.G.). Additional support was provided through grants from the Lille and Alfy Nathan, Barbara Fox Miller, and Wolfson Foundations (to E. G.); by the Horwitz Foundation through the Center for Complexity Science (E. G., R.A., H.B., and Y.E.); and by the Israeli Ministry of Science, Culture, and Sport (Eshkol Scholarship to H.B.).

- Karin M, Greten FR (2005) NF- $\kappa$ B: Linking inflammation and immunity to cancer development and progression. *Nat Rev Immunol* 5:749–759.
- Mantovani A, Allavena P, Sica A, Balkwill F (2008) Cancer-related inflammation. *Nature* 454:436–444.
- O'Byrne KJ, Dalglish AG (2001) Chronic immune activation and inflammation as the cause of malignancy. *Br J Cancer* 85:473–483.
- Kundu JK, Surh YJ (2008) Inflammation: Gearing the journey to cancer. *Mutat Res* 659:15–30.
- Coussens LM, Werb Z (2002) Inflammation and cancer. *Nature* 420:860–867.
- El-Serag HB, Rudolph KL (2007) Hepatocellular carcinoma: Epidemiology and molecular carcinogenesis. *Gastroenterology* 132:2557–2576.
- Umeda T, Hino O (2002) Molecular aspects of human hepatocarcinogenesis mediated by inflammation: From hypercarcinogenic state to normo- or hypocarcinogenic state. *Oncology* 62(Suppl 1):38–42.
- Berasain C, et al. (2009) Inflammation and liver cancer: New molecular links. *Ann NY Acad Sci* 1155:206–221.
- Pikarsky E, et al. (2004) NF- $\kappa$ B functions as a tumour promoter in inflammation-associated cancer. *Nature* 431:461–466.
- Llovet JM (2005) Updated treatment approach to hepatocellular carcinoma. *J Gastroenterol* 40:225–235.
- Schwartz M, Roayaie S, Konstadoulakis M (2007) Strategies for the management of hepatocellular carcinoma. *Nat Clin Pract Oncol* 4:424–432.
- Llovet JM, Schwartz M, Mazzaferro V (2005) Resection and liver transplantation for hepatocellular carcinoma. *Semin Liver Dis* 25:181–200.
- de Jong KP, et al. (1995) The effect of partial hepatectomy on tumor growth in rats: In vivo and in vitro studies. *Hepatology* 22:1263–1272.
- Loizidou MC, et al. (1991) Facilitation by partial hepatectomy of tumor growth within the rat liver following intraportal injection of syngeneic tumor cells. *Clin Exp Metastasis* 9:335–349.
- Asaga T, et al. (1991) The enhancement of tumor growth after partial hepatectomy and the effect of sera obtained from hepatectomized rats on tumor cell growth. *Jpn J Surg* 21:669–675.
- Solt DB, et al. (1983) Promotion of liver cancer development by brief exposure to dietary 2-acetylaminofluorene plus partial hepatectomy or carbon tetrachloride. *Cancer Res* 43:188–191.
- Rizvi TA, Mathur M, Nayak NC (1989) Enhancement of aflatoxin B1-induced hepatocarcinogenesis in rats by partial hepatectomy. *Virchows Arch B Cell Pathol* 56:345–350.
- Hanigan MH, Winkler ML, Drinkwater NR (1990) Partial hepatectomy is a promoter of hepatocarcinogenesis in C57BL/6J male mice but not in C3H/HeJ male mice. *Carcinogenesis* 11:589–594.
- Sarrafi-Yazdi S, Mi J, Dewhirst MW, Clary BM (2008) Use of bioluminescence imaging to detect enhanced hepatic and systemic tumor growth following partial hepatectomy in mice. *Eur J Surg Oncol* 34:476–481.
- Fausto N, Riehle KJ (2005) Mechanisms of liver regeneration and their clinical implications. *J Hepatobiliary Pancreat Surg* 12:181–189.
- Echave Llanos JM, Badrán AF, Moreno FR (1986) Inhibiting effect of a hepatoma extract on the mitotic rate of regenerating liver. *Virchows Arch B Cell Pathol* 51:17–27.
- Echave Llanos JM, Moreno FR, Badrán AF (1986) Inhibiting effect of plasma from normal and tumour bearing mice on the mitotic rate of regenerating liver. *Virchows Arch B Cell Pathol* 52:67–73.
- Mauad TH, et al. (1994) Mice with homozygous disruption of the mdr2 P-glycoprotein gene. A novel animal model for studies of nonsuppurative inflammatory cholangitis and hepatocarcinogenesis. *Am J Pathol* 145:1237–1245.
- Barash H, et al. (2008) Functional magnetic resonance imaging monitoring of pathological changes in rodent livers during hyperoxia and hypercapnia. *Hepatology* 48:1232–1241.
- Katzenellenbogen M, et al. (2007) Molecular mechanisms of liver carcinogenesis in the mdr2-knockout mice. *Mol Cancer Res* 5:1159–1170.
- Katzenellenbogen M, et al. (2006) Multiple adaptive mechanisms to chronic liver disease revealed at early stages of liver carcinogenesis in the Mdr2-knockout mice. *Cancer Res* 66:4001–4010.
- Mochan TA, Venere M, DiTullio RA, Jr, Halazonetis TD (2004) 53BP1, an activator of ATM in response to DNA damage. *DNA Repair* 3:945–952.
- Fillingham J, Keogh MC, Krogan NJ (2006) GammaH2AX and its role in DNA double-strand break repair. *Biochem Cell Biol* 84:568–577.
- Bekker-Jensen S, et al. (2006) Spatial organization of the mammalian genome surveillance machinery in response to DNA strand breaks. *J Cell Biol* 173:195–206.
- Shiloh Y (2006) The ATM-mediated DNA-damage response: Taking shape. *Trends Biochem Sci* 31:402–410.
- Lavin MF (2007) ATM and the Mre11 complex combine to recognize and signal DNA double-strand breaks. *Oncogene* 26:7749–7758.
- Jeggo PA, Löbrich M (2007) DNA double-strand breaks: Their cellular and clinical impact? *Oncogene* 26:7717–7719.
- Shiloh Y (2003) ATM and related protein kinases: Safeguarding genome integrity. *Nat Rev Cancer* 3:155–168.
- Rao VA, et al. (2007) Endogenous gamma-H2AX-ATM-Chk2 checkpoint activation in Bloom's syndrome helicase deficient cells is related to DNA replication arrested forks. *Mol Cancer Res* 5:713–724.
- Brugarolas J, et al. (1999) Inhibition of cyclin-dependent kinase 2 by p21 is necessary for retinoblastoma protein-mediated G1 arrest after gamma-irradiation. *Proc Natl Acad Sci USA* 96:1002–1007.
- Bartkova J, et al. (2005) DNA damage response as a candidate anti-cancer barrier in early human tumorigenesis. *Nature* 434:864–870.
- Ozturk M, Arslan-Ergul A, Bagislar S, Senturk S, Yuzugullu H (2009) Senescence and immortality in hepatocellular carcinoma. *Cancer Lett* 286:103–113.
- Van Gent DC, Hoesjmakers JH J, Kanaar R (2001) Chromosomal stability and the DNA double-strand break connection. *Nat Rev Genet* 2:196–206.
- Carter SL, Eklund AC, Kohane IS, Harris LN, Szallasi Z (2006) A signature of chromosomal instability inferred from gene expression profiles predicts clinical outcome in multiple human cancers. *Nat Genet* 38:1043–1048.
- Farazi PA, DePinho RA (2006) Hepatocellular carcinoma pathogenesis: From genes to environment. *Nat Rev Cancer* 6:674–687.
- Michalopoulos GK (2007) Liver regeneration. *J Cell Physiol* 213:286–300.
- Tarasov V, et al. (2007) Differential regulation of microRNAs by p53 revealed by massively parallel sequencing: miR-34a is a p53 target that induces apoptosis and G1-arrest. *Cell Cycle* 6:1586–1593.
- Zimmermann A (2002) Liver regeneration: The emergence of new pathways. *Med Sci Monit* 8:RA53–RA63.
- Nuciforo PG, Luise C, Capra M, Pelosi G, d'Adda di Fagagna F (2007) Complex engagement of DNA damage response pathways in human cancer and in lung tumor progression. *Carcinogenesis* 28:2082–2088.
- Chaparro M, Sanz-Cameno P, Trapero-Marugan M, Garcia-Buey L, Moreno-Otero R (2007) Mechanisms of angiogenesis in chronic inflammatory liver disease. *Ann Hepatol* 6:208–213.
- Bristow RG, Hill RP (2008) Hypoxia and metabolism. Hypoxia, DNA repair and genetic instability. *Nat Rev Cancer* 8:180–192.
- Aguilera A, Gómez-González B (2008) Genome instability: A mechanistic view of its causes and consequences. *Nat Rev Genet* 9:204–217.
- Celeste A, et al. (2003) H2AX haploinsufficiency modifies genomic stability and tumor susceptibility. *Cell* 114:371–383.
- Zindy P, et al. (2005) Upregulation of DNA repair genes in active cirrhosis associated with hepatocellular carcinoma. *FEBS Lett* 579:95–99.
- Sasaki M, Ikeda H, Nakanuma Y (2008) Activation of ATM signaling pathway is involved in oxidative stress-induced expression of mitogenic-inhibitory p21WAF1/Cip1 in chronic non-suppurative destructive cholangitis in primary biliary cirrhosis: An immunohistochemical study. *J Autoimmun* 31:73–78.
- Teoh NC, et al. (2008) Defective DNA strand break repair causes chromosomal instability and accelerates liver carcinogenesis in mice. *Hepatology* 47:2078–2088.
- Bartkova J, et al. (2006) Oncogene-induced senescence is part of the tumorigenesis barrier imposed by DNA damage checkpoints. *Nature* 444:633–637.
- Halazonetis TD, Gorgoulis VG, Bartek J (2008) An oncogene-induced DNA damage model for cancer development. *Science* 319:1352–1355.
- Higgins GM, Anderson RM (1931) Experimental pathology of the liver. I. Restoration of the liver of the white rat following partial surgical removal. *Arch Pathol* 12:186–202.
- Greene AK, Puder M (2003) Partial hepatectomy in the mouse: Technique and perioperative management. *J Invest Surg* 16:99–102.